

Influence of Chloride and Nitrate Anions on Copper Electrodeposition onto Au(111) from Deep Eutectic Solvents

Tanja Geng,^[a] Benjamin W. Schick,^[a] Matthias Uhl,^[a] Alexander J. C. Kuehne,^[b] Ludwig A. Kibler,^[a] Maximilian U. Cebelin,^{*,[a]} and Timo Jacob^{*,[a, c, d]}

Copper electrodeposition on Au(111) from deep eutectic solvents (DESs) type III was investigated employing cyclic voltammetry as well as chronoamperometry. It was further examined on Au(poly) using the electrochemical quartz crystal microbalance (EQCM). The employed DESs are mixtures of choline chloride (ChCl) or choline nitrate (ChNO₃) with ethylene glycol (EG) as hydrogen bond donor (HBD), each in a molar ratio of 1:2. CuCl, CuCl₂, or Cu(NO₃)₂·3H₂O were added as copper sources. Underpotential deposition (UPD) of Cu precedes bulk deposition in chloride as well as nitrate electrolytes.

Cu deposition from Cu⁺ in chloride media is observed as a one-electron reaction, whereas deposition from Cu²⁺ occurs in two steps since Cu⁺ is strongly stabilized by chloride. Cu⁺ is less stabilized by nitrate and the beginning of bulk deposition in the nitrate-containing DES with Cu²⁺ is shifted by several hundred mV to more positive potentials compared to the chloride DES. A diffusion-controlled, three-dimensional nucleation and growth mechanism is found by chronoamperometric measurements and analysis based on the model of Scharifker and Mostany.

Introduction

The electrodeposition of copper is applied on a large industrial scale in producing printed circuit boards and electronic components. In particular, the production of very fine structures and thin layers is of high interest because Cu is used to connect the individual electronic elements.^[1–3] The copper-damascene process even allows the deposition of structures with sizes down to the nanoscale for high-tech applications. However, the fabrication of structures with dimensions of less than 10 nm cannot be achieved yet, as it requires a defect-free copper layer.^[4] Here, the galvanic bath plays a crucial role since copper should be plated as efficiently as possible, in other words, with

minimal leakage currents and at high deposition rates without incorporating impurities. To actively influence the properties of electrodeposited structures, a detailed understanding of the initial stages of electrodeposition is indispensable.

Perhaps even triggered by its technological importance, electrochemical copper deposition has become one of the best-investigated processes and is highly important in fundamental research. For this reason, a plethora of literature is devoted to the fundamentals of metal deposition, including underpotential deposition, nucleation and growth processes, and the effects of additives.^[5–10] Further, the electrolyte, which can be of aqueous or non-aqueous nature, plays an important role. Among other aspects, these studies have helped to gain a general understanding of the deposition behavior on different electrode surfaces and thus have contributed to technological progress in industry, for example in the development of coatings with the respective desired properties.

Deep eutectic solvents (DESs) are a class of water-free electrolytes that can be produced from environmentally friendly substances. Sustainability is becoming increasingly important also in electrodeposition, and there is an urgent need for environmentally friendly electrolytes due to ever-stricter safety and health regulations. In general, DESs are binary mixtures of an ionic compound with another ionic compound or a hydrogen bond donor. They are distinguished into four different types, with types III and IV being the most important.^[11] Here, either an organic (type III) or a metal salt (type IV) is combined with a polar organic hydrogen bond donor molecule.

To better understand the influence and potential of DESs as a new class of electrolytes,^[12–14] the present study concentrates on the benchmarking process of copper electrodeposition on clean and well-defined electrode surfaces. The present work focuses on DESs type III with the addition of copper salts in

[a] T. Geng, B. W. Schick, M. Uhl, Dr. L. A. Kibler, Dr. M. U. Cebelin, Prof. Dr. T. Jacob
Institute of Electrochemistry
Ulm University
Albert-Einstein-Allee 47, 89081 Ulm, Germany
E-mail: maximilian.cebclin@uni-ulm.de
timo.jacob@uni-ulm.de

[b] Prof. Dr. A. J. C. Kuehne
Institute of Organic and Macromolecular Chemistry
Ulm University
Albert-Einstein-Allee 11, 89081, Ulm, Germany

[c] Prof. Dr. T. Jacob
Helmholtz-Institute Ulm (HIU) for Electrochemical Energy Storage
Helmholtzstr. 11, 89081 Ulm, Germany

[d] Prof. Dr. T. Jacob
Karlsruhe Institute of Technology (KIT)
P.O. Box 3640, 76021 Karlsruhe, Germany

 Supporting information for this article is available on the WWW under <https://doi.org/10.1002/celec.202101263>

 © 2022 The Authors. ChemElectroChem published by Wiley-VCH GmbH. This is an open access article under the terms of the Creative Commons Attribution Non-Commercial NoDerivs License, which permits use and distribution in any medium, provided the original work is properly cited, the use is non-commercial and no modifications or adaptations are made.

contact with an Au(111) single crystal model electrode. In contrast to silver deposition from DESs,^[15,16] the two possible oxidation states of copper cations entail more complex behavior, which might be transferable to other multivalent metal ions. Moreover, other metals, such as aluminum and nickel, show better conductivity at very small dimensions compared to their bulk deposits. For these non-noble metals, a water-free electrolyte bath will be advantageous.

Several studies on copper deposition from DESs precede this work. First, composite materials based on copper were deposited from a DES of choline chloride (ChCl) mixed with urea or ethylene glycol (EG) and CuCl₂ on platinum electrodes, where different kinetics and thermodynamics than in aqueous solutions were found.^[14] The authors ascribed this to a different complexation of the copper ions, which is to be expected due to the relatively high chloride concentration and the low water content. With a higher water content, the mass transfer of Cu²⁺ in a DES of ChCl/EG is increased.^[17] A complexation of Cu⁺ by chloride ligands connected with strong stabilization was also found in a ChCl/urea DES with CuCl₂ in contact with a glassy carbon electrode.^[18,19] However, so far there is little knowledge about Cu electrodeposition on Au(*hkl*) single crystal electrodes from DESs. One study focused on underpotential deposition, but only the typical chloride-based DES with urea was investigated.^[20] In combination with single crystal electrodes, EG as hydrogen bond donor (HBD) has only been applied in two recent studies. The morphology of Cu nuclei deposited from ChCl/EG with CuCl₂ on Au(111) and the adsorption structure on top of the nuclei was elucidated by *in-situ* scanning tunneling microscopy (STM).^[21] If the molar ratio of ChCl to EG is altered, the diffusion rates of Cu⁺ as well as Cu²⁺ change due to differences in viscosity of the mixtures.^[22] The same behavior was found for mixtures of ChCl with trifluoroacetamide (TFA) as HBD.

Yet, the role of chloride and other anions present in high concentration in Cu electrodeposition is still unclear and has not been studied in detail. In this work on Cu deposition onto Au(111) and Au(poly), ethylene glycol is combined with choline chloride or choline nitrate to compare their different deposition behavior with the addition of Cu⁺ or Cu²⁺ sources. The electrochemical behavior of the metal-free binary mixtures is also addressed. Nitrate as anion is chosen as it is widely applied in Cu deposition from aqueous media, and choline nitrate can be synthesized relatively easily. By cyclic voltammetry and electrochemical quartz crystal microbalance (EQCM), we investigate underpotential and overpotential processes and resolve the reactions during deposition and dissolution, focusing on differences between chloride- and nitrate-containing electrolytes. The results are supplemented by chronoamperometry to gain deeper insight into nucleation and growth from this type of electrolytes. An important aspect of this work is to compare the roles of water and ethylene glycol as solvents by identifying similarities and differences to Cu deposition from aqueous electrolytes.

Results and Discussion

The ChCl/EG DES is prepared in the commonly used molar ratio of 1:2 ($x_{\text{ChCl}}=0.33$) as it is beneficial for comparison with literature. However, it has been shown by differential scanning calorimetry (DSC) that the eutectic ratio is 16:84 ($x_{\text{ChCl}}=0.16$).^[22] For a better comparison of the electrolytes, a molar ratio of 1:2 is also used for choline nitrate ChNO₃/EG.

Cyclic Voltammetry

In Figure 1a, cyclic voltammograms are presented for an Au(111) single crystal electrode in ChCl/EG ($x_{\text{ChCl}}=0.33$) with 20 mM CuCl with window-opening to negative potentials from one cycle to the next. The positive potential limit has been set to 0.7 V_{Cu} to prevent the oxidation of Cu⁺ to Cu²⁺. Three peaks appear between 0.6 and 0.7 V_{Cu} close together with their respective counter peaks. The cathodic and anodic charge densities in this potential region are $-150 \mu\text{C cm}^{-2}$ and $170 \mu\text{C cm}^{-2}$, respectively. It becomes apparent that these three peaks are related to the presence of Cu when comparing the

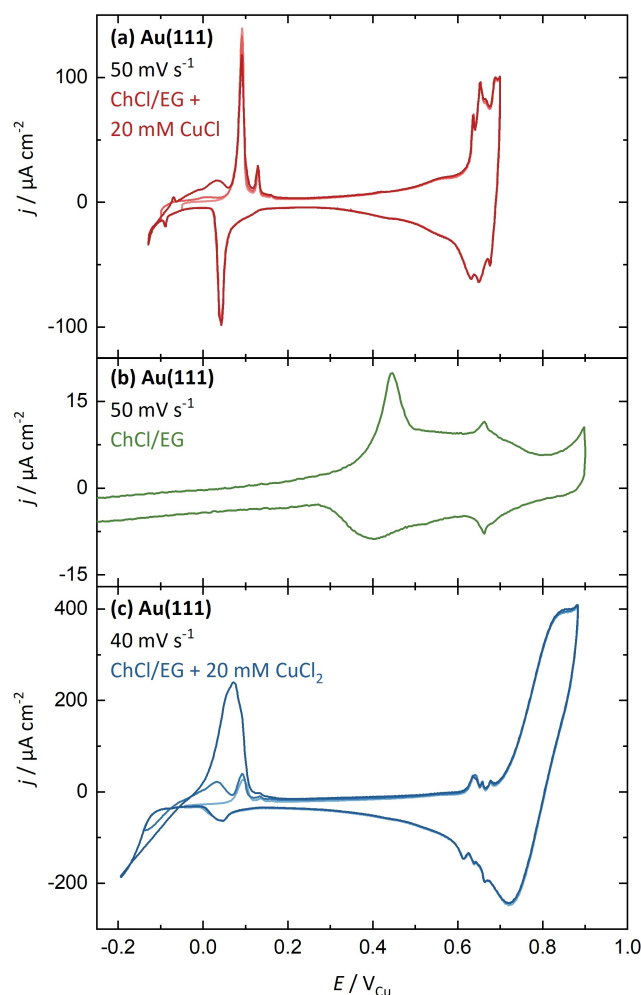


Figure 1. Cyclic voltammograms of Au(111) in DES of (a) ChCl/EG with 20 mM CuCl, (b) pure ChCl/EG, and (c) ChCl/EG with 20 mM CuCl₂.

cyclic voltammogram with the one on Au(111) in the DES base electrolyte (Figure 1b). Au(111) in the Cu-ion-free electrolyte exhibits peaks corresponding to chloride adsorption, but with lower current densities and the most prominent peak being at $0.4 V_{Cu}$. Therefore, we expect the initial stages of Cu underpotential deposition (UPD) to occur around $0.6 V_{Cu}$, probably including adsorption of chloride on the UPD layer. Very similar behavior has previously been reported for Au(*hkl*) single crystal electrodes in DESs with different HBDs, namely in ChCl/urea^[20] and ChCl/TFA mixtures.^[22]

Stepwise extension of the negative potential limit reveals a process starting at $0.15 V_{Cu}$ with a sharp cathodic peak around $0.05 V_{Cu}$, which exhibits two anodic counter-peaks in the positive scan (Figure 1a). These are signs of the second part of Cu UPD with a charge density of approximately $-50 \mu C cm^{-2}$ and $50 \mu C cm^{-2}$, respectively, corresponding to the deposition of 0.23 monolayers of Cu. Since the formation of the Cu UPD layer begins already at more positive potentials, we assume the completion of the first Cu monolayer here. The total transferred charge densities ($-200 \mu C cm^{-2}$ and $220 \mu C cm^{-2}$) are close to the theoretically expected value of $222 \mu C cm^{-2}$ for deposition and dissolution of one monolayer without anion and capacitive effects. The anodic charge density is higher than the cathodic since the oxidation of Cu^+ to Cu^{2+} is probably already occurring at a low rate.

Similar behavior is known for copper deposition onto gold single crystals in chloride-containing aqueous^[23] and other non-aqueous electrolytes.^[10] However, the two stages of the UPD process are located closer to each other in aqueous electrolytes. *In-situ* STM measurements have shown that a commensurate (5×5) Cu structure is formed after the first deposition peak in the presence of chloride.^[8,9,23] The Cu coverage on the Au(111) surface is 0.62 ML with one chloride molecule adsorbed to each Cu atom forming a bilayer structure.^[9,24,25] In aqueous electrolytes, the second UPD peak occurs just positive of bulk deposition and is ascribed to the completion of the first monolayer.^[23] In the ChCl/EG DES, this process is followed by two small peaks at around $-0.08 V_{Cu}$, which might be caused by adsorbed chloride, and the bulk deposition of copper starting at $-0.1 V_{Cu}$. The dissolution of the deposited layer starts, as expected, around $0 V_{Cu}$. The dissolution of the UPD layer is observed separately and occurs in two steps, 450 mV apart. The first step starts slightly positive of Cu bulk dissolution and is followed by the second one positive of $0.6 V_{Cu}$.

With $CuCl_2$ as a copper source (Figure 1c), the cyclic voltammograms on Au(111) were recorded with a positive potential limit of $0.88 V_{Cu}$ to avoid chloride-induced Au dissolution. Between 0.7 and $0.8 V_{Cu}$ a redox peak occurs that is attributed to the redox reaction between Cu^{2+} and Cu^+ .^[26] This process is also observed for other chloride-containing aqueous^[27,28] and non-aqueous electrolytes.^[14,18,26] However, for example it has also been detected in a chloride-free aqueous solution of $50 \text{ mM } Cu(NH_3)_4^{2+} + 1 \text{ M } NH_3 + 1 \text{ M } NaNO_3$ at pH 10.5.^[27] Generally, it takes place positive of the Cu overpotential deposition (OPD) if its equilibrium potential in the respective electrolyte is higher than that of the OPD due to stabilization of Cu^+ in the electrolyte. Otherwise, only a

deposition peak is observable in which two electrons are transferred, e.g., in sulfate electrolytes.^[29] If the Cu^+/Cu^{2+} redox peak occurs and Cu^+ is stable in the electrolyte, the potential separation to the OPD depends on the nature and composition of the electrolyte. It can reach up to several hundred mV in chloride-containing electrolytes, depending on the chloride concentration.^[6,18,28] This separation is therefore also very pronounced for various electrodes in contact with chloride-containing DESs due to strong Cu^+ stabilization.^[18,30–33] The less water is present in the electrolyte, the more separated are the Cu^{2+}/Cu^+ redox peak and OPD, i.e., the higher is the stabilization of Cu^+ .^[17,34] The stabilization is due to the formation of Cu(I) chloride complexes, leading to a higher formal potential of the Cu^+/Cu^{2+} redox process and a negative shift of the equilibrium potential of Cu bulk deposition/dissolution. Cu^{2+} is predominantly present as $[CuCl_4]^{2-}$ for high chloride concentrations.^[14,17,30,33–35] For Cu^+ , the prevailing species are $[CuCl_3]^{2-}$ ^[26] and $[CuCl_2]^-$.^[35,36]

Between 0.6 and $0.7 V_{Cu}$, three small peaks can be seen in Figure 1c, as in the case of the Cu^+ system (Figure 1a). Due to the overlap with the Cu^+/Cu^{2+} peak, their charge density cannot easily be determined. At $0.05 V_{Cu}$, again, a peak with a charge density of around $50 \mu C cm^{-2}$ is observed. Since these two processes occur at the same potential and have a similar charge density as with CuCl, we assume the same behavior in both electrolytes: formation of a UPD monolayer in two steps, followed by bulk deposition negative of $-0.1 V_{Cu}$. The similar charge densities point to the fact that in both cases, UPD takes place by a one-electron reduction of Cu^+ , which has previously been produced in the $CuCl_2$ -containing electrolyte.

Figure 2 shows cyclic voltammograms of Au(111) in a nitrate-containing DES: choline nitrate and ethylene glycol without (green curve) and with (orange curve) 20 mM $Cu(NO_3)_2$. Au(111) in the copper-free electrolyte does not exhibit characteristic peaks in the potential window between 0 and $0.85 V_{Cu}$, which is also the case for aqueous nitrate-containing

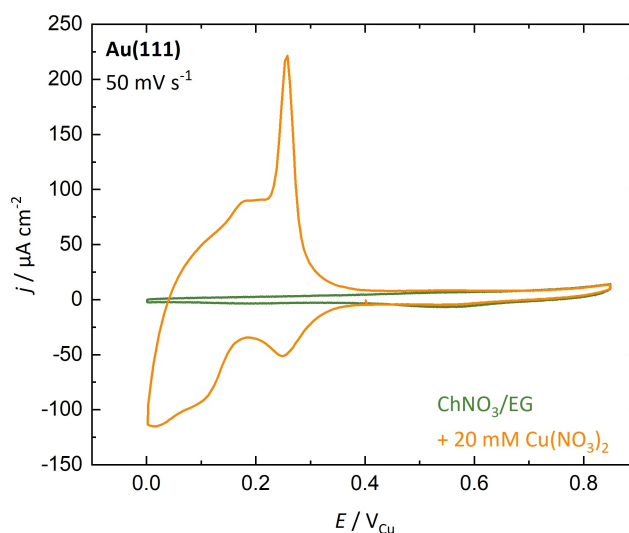


Figure 2. Cyclic voltammograms of Au(111) in ChNO₃/EG (green) and with 20 mM Cu(NO₃)₂ (orange) at a scan rate of 50 mV s^{-1} from 0 to $0.85 V_{Cu}$.

electrolytes.^[37] However, there are remarkable differences between nitrate- and chloride-based DESs in the cyclic voltammograms after adding Cu^{2+} salt. For the nitrate-based DES, the $\text{Cu}^+/\text{Cu}^{2+}$ redox process is absent positive of the UPD, in contrast to the electrolyte with CuCl_2 (Figure 1c). A detailed explanation of this observation is given in the EQCM section below, however, it already suggests that Cu^+ species are not as stabilized by nitrate as they are by chloride. Like the chloride system, the DES with $\text{Cu}(\text{NO}_3)_2$ also shows peaks that can be attributed to UPD. There are two cathodic and two corresponding anodic peaks positive of $0 V_{\text{Cu}}$ that convert a charge density of $-420 \mu\text{Ccm}^{-2}$ and $410 \mu\text{Ccm}^{-2}$. This corresponds to the formation of one copper monolayer on the Au(111) surface for a two-electron reduction. It is well-known that the nature of the anions may affect the Cu UPD thermodynamically and kinetically.^[23] This is well-established for sulfate,^[8] halides,^[9,24,25] and perchlorate^[23] in aqueous electrolytes. Interestingly, Cu UPD on Au(111) has not been observed for aqueous nitrate solutions. Nevertheless, it is detected in this DES, although nitrate does not show specific adsorption on Au(111), according to the cyclic voltammogram.

To gain a better understanding of the differences between the chloride and nitrate systems, Cu bulk deposition on Au(111) in the ChCl/EG DES with CuCl or CuCl_2 is presented in Figure 3a. Au(111) in the CuCl electrolyte (red curve) was only cycled up to a potential of $0.5 V_{\text{Cu}}$ to avoid oxidation to Cu^{2+} . Negative of $0 V_{\text{Cu}}$, in the potential region of bulk deposition, the main feature is observable at $-0.2 V_{\text{Cu}}$ followed by two other processes occurring to a lesser extent. These do not take place

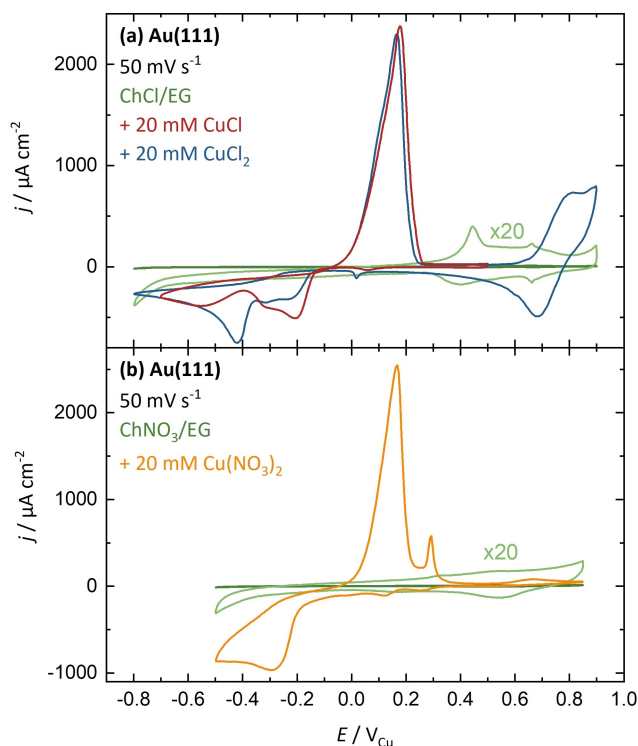


Figure 3. Cyclic voltammograms of Au(111) in (a) ChCl/EG (green) with 20 mM CuCl (red) or 20 mM CuCl_2 (blue) and (b) Ch NO_3 /EG (green) with 20 mM $\text{Cu}(\text{NO}_3)_2$ (orange) at a scan rate of 50 mVs^{-1} .

in the Cu-ion-free ChCl/EG DES, neither on Au(111) (green curve in Figure 3a) nor on Cu.^[38,39] On Cu, ChCl/EG is stable until $-0.9 V_{\text{Ag/AgCl}}$ ^[38,39] which in this case corresponds to approximately $-0.7 V_{\text{Cu}}$. So, the cathodic decomposition of the DES on Au(111) and Cu starts at similar potentials. In the relevant potential window, ChCl/EG is stable and the processes observable with CuCl (red curve in Figure 3a) are related to copper. The charge density associated with the three cathodic features in the CuCl electrolyte is -5.64 mCcm^{-2} and 5.62 mCcm^{-2} for dissolution, implying a Coulombic efficiency of 99.7% and indicating deposition from Cu^+ and dissolution to Cu^+ rather than directly to Cu^{2+} . Two possible reasons for the three deposition peaks are the nature of the Au(111) substrate and the deposition proceeding from different copper(I) chloride complexes with different redox potentials. It is known that the redox potentials of Cu species depend on the complexation of Cu ions in aqueous electrolytes.^[40,41] However, it is unusual that several deposition processes are observed in one system. Moreover, the presence of EG might affect the deposition potential and the exchange current density. With water as the solvent, poly(ethylene glycol) (PEG) is often added as an inhibitor in combination with chloride, since PEG adsorbs on the Cu surface and a PEG–Cu–Cl complex is formed.^[42] Therefore, it cannot be excluded that EG is part of a similar complex. If the scan rate is lower (5 mVs^{-1}), a single peak is observed in the OPD region at $-0.13 V_{\text{Cu}}$ (red curve in Figure S1). Thus, the additional peaks observed at a higher scan rate of 50 mVs^{-1} at more negative potentials are caused by kinetic effects.

In the electrolyte with CuCl_2 (blue curve in Figure 3a), the peak at $-0.2 V_{\text{Cu}}$ is also observed, albeit smaller, and a cathodic peak at $-0.4 V_{\text{Cu}}$ is dominant. The Coulombic efficiency of 88.0% (-6.06 mCcm^{-2} and 5.33 mCcm^{-2}) is lower than with Cu^+ . The negative charge density is larger because, at potentials negative of the $\text{Cu}^+/\text{Cu}^{2+}$ redox couple, the reduction of Cu^{2+} to Cu^+ takes place constantly. Also, a currentless dissolution by comproportionation of Cu with Cu^{2+} to Cu^+ is possible, as observed previously in a ChCl/EG DES.^[17] As both phenomena result in the same charge, the combination of electrochemical and EQCM measurements proves beneficial in this case (see below). During cycling (Figure S2), the peak current density of the first peak increases, and that of the second peak decreases. A deposition peak at $-0.4 V_{\text{Cu}}$ that diminishes with cycling has also been observed in a ChCl/TFA DES with CuCl_2 for a high chloride concentration ($x_{\text{ChCl}}=0.4$).^[22] For a lower scan rate (5 mVs^{-1}), both peaks occur but to a similar extent (blue curve in Figure S1). In contrast to Au(111), a single peak is observed for Au(poly) (blue curve in Figure 4a), as in the case of CuCl (red curves in Figures S1 and 4a). Thus, it is supposed that the well-ordered structure of the Au(111) surface leads to the additional peak at $-0.4 V_{\text{Cu}}$.

In Figure 3b, cyclic voltammograms of the Ch NO_3 /EG DES are depicted. Au(111) in the copper-free electrolyte (green curve) does still not show characteristic peaks. With $\text{Cu}(\text{NO}_3)_2$ (orange curve) there are unique features for copper deposition compared to the chloride-based DES with CuCl_2 . Although Cu^{2+} species are present in both electrolytes, only a single deposition peak starting at $-0.2 V_{\text{Cu}}$, i.e., with quite some overpotential, is

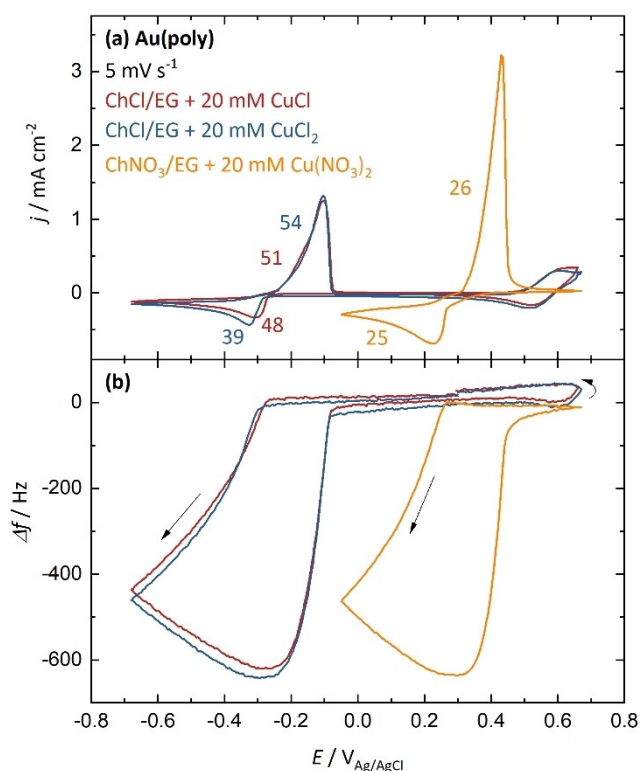


Figure 4. (a) Cyclic voltammetry coupled with EQCM of a gold-coated quartz crystal at a scan rate of 5 mV s^{-1} in ChCl/EG with 20 mM CuCl (red), ChCl/EG with 20 mM CuCl₂ (blue), and ChNO₃/EG with 20 mM Cu(NO₃)₂ (orange) vs. an Ag/AgCl reference electrode. The values given are the M/z values calculated for the respective processes. (b) Corresponding change in frequency as a function of potential for the three different electrolytes.

visible. However, the current already starts to decrease around 0 V_{Cu} , indicating a second reaction. These reactions are further characterized by EQCM. Negative of $-0.4 \text{ V}_{\text{Cu}}$, the current stays approximately constant as another process starts. This process seems to be irreversible since the Coulombic efficiency over the whole potential range is rather low (71% with -8.56 mC cm^{-2} and 6.09 mC cm^{-2}). If the vertex potential is less negative (red curve in Figure S3) and this process is omitted entirely, the Coulombic efficiency is very high (99.9% with -2.90 mC cm^{-2} and 2.89 mC cm^{-2}). Copper dissolution of the bulk layers and the UPD layer are separated and distinguishable. The charges involved in the UPD are quite similar for different negative reversal potentials, although the peak height in the cyclic voltammograms is different (compare Figure 2 and 3b). In more detail, this can be seen in a window-opening experiment (Figure S3).

Electrochemical Quartz Crystal Microbalance

EQCM measurements were performed to provide a deeper insight into the electrodeposition and dissolution behavior of the three copper-containing electrolytes. During cyclic voltammetry and chronopotentiometry experiments, the resonance frequency of a 5 MHz quartz crystal coated with polycrystalline

gold, which served as a working electrode at the same time, was recorded. The cyclic voltammograms presented in Figure 4a were conducted with a leak-free Ag/AgCl reference electrode at a scan rate of 5 mV s^{-1} . The $\text{Cu}^+/\text{Cu}^{2+}$ redox peak, as well as deposition and dissolution, are each observed at approximately the same potentials in both chloride-based electrolytes. The deposition/dissolution for the nitrate-based electrolyte takes place roughly 550 mV positive compared to the chloride-containing electrolytes. The fact that a significantly more negative potential is necessary to deposit Cu from chloride-containing electrolytes and that Cu^+ is formed easily further emphasizes the high stability of Cu^+ due to complex formation in these systems, as previously discussed. By contrast, Cu^+ seems to be only slightly stabilized by nitrate. Compared to the cyclic voltammograms for Cu deposition on Au(111) (Figure 3), the peaks corresponding to UPD are very broad and are therefore hardly recognizable on polycrystalline Au (Figure 4a).

Figure 4b shows the change in frequency Δf of the Au-coated quartz crystal providing additional information to the electrochemical measurements in Figure 4a. According to the Sauerbrey equation, the change in frequency is proportional to the change in mass of the quartz.^[43] During deposition, the frequency decreases by about 600 Hz in all cases, which means that the same amount of Cu is deposited on the gold electrode. While Cu is dissolved, the frequency increases to its initial value, thus confirming the high reversibility of this process. For the DESs with chloride salts (red and blue curves), no change in frequency is observable at potentials between 0.4 and $0.6 \text{ V}_{\text{Ag/AgCl}}$, matching well with the assumption that these peaks in the cyclic voltammogram correspond to the $\text{Cu}^+/\text{Cu}^{2+}$ redox process. Since this process occurs in solution, no significant mass change on the electrode is detectable. At more positive potentials, starting at $0.62 \text{ V}_{\text{Ag/AgCl}}$, the frequency increases, which fits well with the expected chloride-induced Au dissolution leading to a mass loss. Au is redeposited partly during the negative scan, but the frequency does not reach its initial value. Looking more closely at Cu deposition in the nitrate-based electrolyte (orange curve), one can see that the sharp current decrease – indicating the beginning of deposition – is preceded by a flatter current decay without change in frequency until $0.27 \text{ V}_{\text{Ag/AgCl}}$.

To specify the deposition and dissolution, the Sauerbrey equation^[43] is combined with Faraday's law to calculate M/z values.^[44] These give the molar mass M of the deposited or dissolved species divided by the number of electrons z , which are transferred in that process [Equation (1)].

$$\frac{M}{z} = -\frac{FA\sqrt{\rho_q\mu_q}}{2f_0^2} \frac{df}{dQ} \quad (1)$$

Hereby, F is the Faraday constant, A the electrochemically active surface area, ρ_q the density of the quartz, μ_q the shear modulus of the quartz, and f_0 the resonance frequency of the quartz. For Cu, one expects the molar mass ($M = 63.5 \text{ g mol}^{-1}$) as M/z value for the reduction of Cu^+ to Cu as well as the oxidation of Cu to Cu^+ ($z = 1$). For a process involving two

electrons ($z=2$), half the value of the molar mass is expected (31.8 g mol^{-1}). That process can either be a reaction of Cu^{2+} to Cu or vice versa, or the same net reactions taking place in two steps in quick succession with Cu^+ as intermediate. M/z values attributed to the deposition and dissolution of Cu are given in Figure 4a for the three electrolytes. These are calculated by determining the slope in f vs. Q diagrams (Figures S4–S6).

As the M/z values for the nitrate-based electrolyte are about half of those for the chloride-containing electrolytes, it is apparent that the deposition occurs by a one-electron transfer from Cu^+ to Cu in both chloride-containing electrolytes. The previously necessary reduction of Cu^{2+} to Cu^+ already starts to occur at much more positive potentials ($0.6 V_{\text{Ag}/\text{AgCl}}$). The value of M/z for the CuCl_2 electrolyte during deposition is 9 g mol^{-1} lower than for the CuCl electrolyte. Similar to the different charge densities in the cyclic voltammogram (Figure S7), this behavior can be explained by the reduction of Cu^{2+} to Cu^+ occurring simultaneously to the deposition but not leading to a change in mass. This lowers the slope df/dQ (Figure S5) leading to a lower M/z value. For the same reason, the M/z value is higher for the CuCl_2 electrolyte than for the CuCl electrolyte during dissolution. The reduction of Cu^{2+} contributes a negative current, which means that the current caused by Cu dissolution is higher than measured. This leads to a higher slope and resulting M/z value. Likewise, this can be regarded as a comproportionation of Cu with Cu^{2+} to Cu^+ , which is a currentless dissolution, occurring to a small extent.

For Cu deposition and dissolution of roughly the same amount of Cu in nitrate and chloride electrolytes, the charge densities are higher in the nitrate- than in the chloride-containing ones (Figure S7). This is also reflected in about twice as high maximum current densities of the cyclic voltammogram (Figure 4a) and in the half as high M/z value with nitrate. Therefore, in contrast to the chloride systems, two electrons are transferred for Cu deposition as well as for dissolution in the nitrate-containing DES.

For all three electrolytes, the experimentally obtained M/z values are lower than the theoretically expected values. One expects 63.5 g mol^{-1} ($z=1$) with CuCl and 31.8 g mol^{-1} ($z=2$) with $\text{Cu}(\text{NO}_3)_2$, from which the obtained values deviate by 18–24%. With CuCl_2 , also $z=1$ is expected but the continuous formation of Cu^+ makes it difficult to state a deviation. As can be seen exemplarily when comparing the M/z values in Figures 4 and 5 for the Cu^+ DES, this deviation is a systematic phenomenon and becomes more pronounced with increasing absolute current density.

The EQCM chronopotentiometry measurement with CuCl (red curve in Figure 5) was recorded at a current density of $-20 \mu\text{A cm}^{-2}$, which is less negative than the deposition current during cyclic voltammetry (red curve in Figure 4a). After 60 s at the open circuit potential (OCP), a current of $-20 \mu\text{A cm}^{-2}$ was applied and the potential was recorded against a Cu wire reference electrode. In the CuCl electrolyte, the OCP is determined by Cu deposition/dissolution and slowly approaches $0 V_{\text{Cu}}$. The OCP is slightly higher in the nitrate-containing DES because it is most likely set by the $\text{Cu}^{2+}/\text{Cu}^+$ redox process, which is further discussed below. The frequency

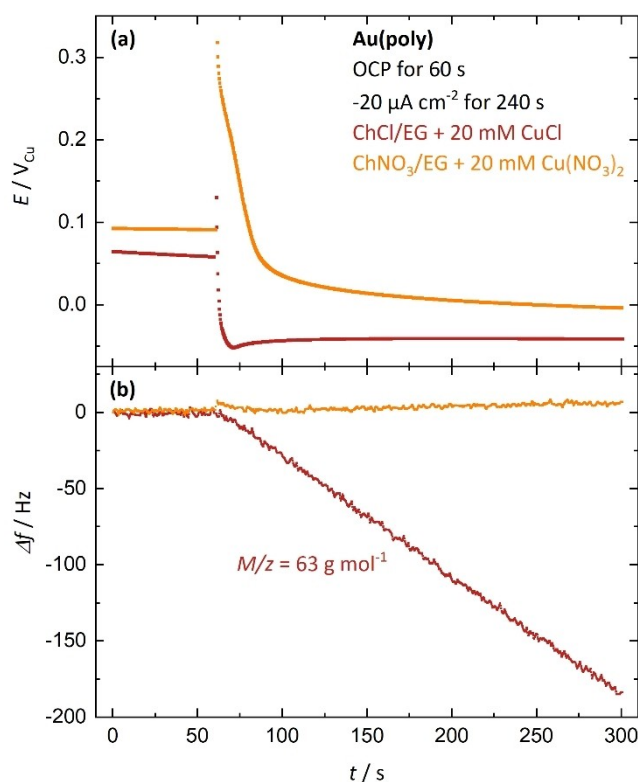


Figure 5. Chronopotentiometric EQCM measurements of a gold-coated quartz crystal in ChCl/EG with 20 mM CuCl (red) and ChNO_3/EG with 20 mM $\text{Cu}(\text{NO}_3)_2$ (orange). After 60 s OCP measurement, $-20 \mu\text{A cm}^{-2}$ were applied for four minutes. In (a), potential vs. time, and in (b), change in frequency vs. time is depicted.

(Figure 5b) during OCP is stable for both the CuCl- and $\text{Cu}(\text{NO}_3)_2$ -electrolyte. It has to be stated that between the OCP measurement and the chronopotentiometry at $-20 \mu\text{A cm}^{-2}$, the potential must have jumped to a value higher than OCP for a very short time as the potential curve starts positive of OCP (Figure 5a). When a negative current is applied to the system with CuCl, UPD is completed fast and the potential drops below $0 V_{\text{Cu}}$. It stabilizes at a constant potential after a small negative overpotential, which is typical for metal deposition.^[45] At the same time, the frequency (red curve in Figure 5b) decreases linearly implying a constant mass change of the electrode. The corresponding M/z value of 63 g mol^{-1} corresponds to the molar mass of copper for a one-electron reduction, as expected for Cu deposition from Cu^+ .

Compared to this, the behavior of the nitrate electrolyte (orange curve in Figure 5) is completely different. The potential drops to a plateau around $0 V_{\text{Cu}}$ when applying $-20 \mu\text{A cm}^{-2}$, and no change in frequency is observed during the 4 minutes of chronopotentiometry measurement. We conclude that Cu deposition does not occur and the total current flow during this time must be caused by another process. Since the transferred charge density of -4.8 mC cm^{-2} is considerably higher than that expected for surface processes such as double-layer charging, adsorption processes, or UPD, it is most likely that Cu^{2+} is reduced to Cu^+ at these potentials. The reference potential of the Cu reference electrode is given by reversible Cu deposition/

dissolution and the measured potential is above $0 V_{Cu}$ for most of the time (orange curve in Figure 5a), which strongly supports the existence of a bulk process.

A chronopotentiometry experiment with a ten times higher current density (Figure 6) compares the behavior of the chloride and nitrate systems with Cu^{2+} . Again, the frequency is stable during the OCP measurement for both electrolytes. In the case of the electrolyte with $CuCl_2$, the OCP is around $0.75 V_{Cu}$ set by the Cu^+/Cu^{2+} redox couple. When applying $-200 \mu A cm^{-2}$ (marked by the vertical grey line in Figure 6), the frequency at first stays constant for both systems. The process starting below $0.75 V_{Cu}$ for the chloride-containing DES (blue curve in Figure 6) is assigned to the reduction of Cu^{2+} to Cu^+ . With nitrate (orange curve), the potential decreases slowly while the frequency is constant, and the same process is assumed to occur. When the potential drops below $0 V_{Cu}$, there is a distinct plateau in both potential profiles associated with a decrease in frequency. At these potentials, two processes are running simultaneously: reduction of Cu^{2+} to Cu^+ and reduction of Cu^+ to Cu. Thus, the M/z values given in Figure 6b fit the molar mass of Cu with $z=2$. However, based on EQCM measurements alone, it cannot directly be stated whether the deposition occurs in a single step from Cu^{2+} to Cu or via a two-step process with Cu^+ as an intermediate. However, in the light of the results discussed above, the direct deposition can be

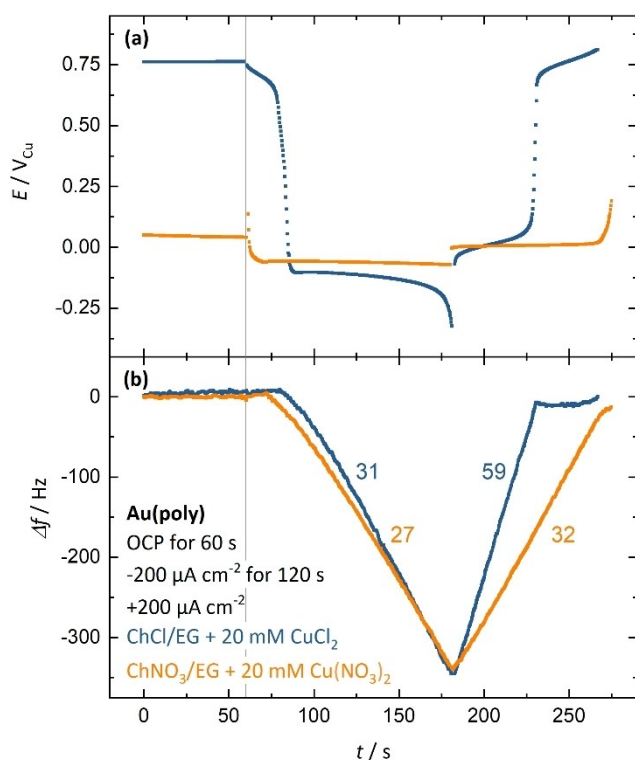


Figure 6. Chronopotentiometric EQCM measurements of a gold-coated quartz crystal in $ChCl/EG$ with $20 \text{ mM } CuCl_2$ (blue) and $ChNO_3/EG$ with $20 \text{ mM } Cu(NO_3)_2$ (orange). After 60 s OCP measurement, $-200 \mu A cm^{-2}$ were applied for two minutes followed by applying a current density of $+200 \mu A cm^{-2}$. In (a), potential vs. time, and in (b), change in frequency vs. time is depicted. The values given are the M/z values calculated for the respective processes.

excluded for the $CuCl_2$ electrolyte and is rather improbable for the $Cu(NO_3)_2$ electrolyte. The M/z value for the nitrate-based electrolyte is slightly lower than for the chloride-based electrolyte. This is because of the higher amount of Cu^+ produced in the first process in the chloride electrolyte. As more Cu^+ is present already, the charge to deposit the same amount of Cu is lower. Comparing Cu deposition measured by cyclic voltammetry (Figure 4) to the galvanostatic measurement at $-200 \mu A cm^{-2}$ (Figure 6), the M/z values are similar for the nitrate-containing electrolyte but different for the chloride-containing system. The lower value in the chronopotentiometry measurement with $CuCl_2$ is related to the shorter time in which Cu^{2+} is reduced to Cu^+ . Therefore, the value is closer to the expected value for a two-electron process.

The M/z value for the dissolution at $+200 \mu A cm^{-2}$ (Figure 6) is different for the two electrolytes and is consistent with the results obtained from cyclic voltammetry (Figure 4). For the nitrate-containing electrolyte, the value corresponds to a two-electron process from Cu to Cu^{2+} . The M/z value being slightly higher for dissolution than for deposition is an indication for continuous reduction of Cu^{2+} to Cu^+ or comproportionation, similar to $CuCl_2$. This observation implies that Cu^+ is also stabilized by nitrate. A further hint for the stabilization of Cu^+ in the nitrate electrolyte is found in another EQCM measurement (Figure S8). Although no net current flows, Cu is dissolved probably by comproportionation with Cu^{2+} to Cu^+ . As the DES might be slightly acidic, it is also possible that Cu dissolution by nitric acid takes place simultaneously. Nevertheless, based on the results presented above, it is concluded that Cu^+ is stable in the nitrate-containing DES and acts as an intermediate both in Cu deposition and dissolution. By contrast, M/z for the chloride electrolyte (Figure 6) fits a one-electron process implying that much less charge is transferred during dissolution than in the nitrate electrolyte. Indeed, this is observable in the potential profile (blue curve in Figure 6a) with the potential rising from around 0 to $0.75 V_{Cu}$ already after 50 seconds of dissolution. After the oxidation of Cu to Cu^+ , an additional plateau is present where the second part of the charge is transferred by subsequent oxidation of Cu^+ to Cu^{2+} . Thus, as with nitrate, the overall oxidation takes place from Cu to Cu^{2+} with Cu^+ as a stable intermediate, but the two steps are further separated.

Chronoamperometry

To elucidate the nucleation and growth mechanism of Cu on Au(111) from these DESs, current transients were recorded after potential steps to a series of constant potentials (in Figure 7, the transients are shown as recorded). For the system with $CuCl_2$, the initial potential was set to $0.83 V_{Cu}$ to prevent Cu^+ formation before the potential step. It was considered important to ensure that initially, no Cu^+ is present. A starting potential of $0.5 V_{Cu}$ was chosen for the $Cu(NO_3)_2$ - and $CuCl$ -containing electrolytes to have similar starting conditions in all systems and to prevent the formation of Cu^{2+} positive of $0.6 V_{Cu}$ in the latter.

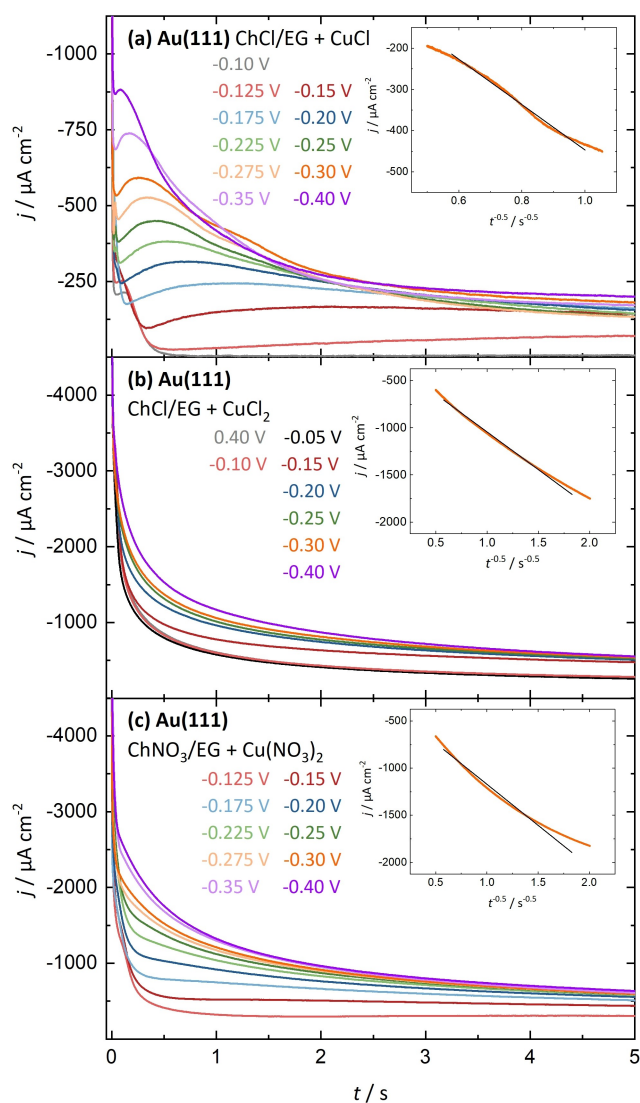


Figure 7. Potentiostatic current transients of Au(111) in (a) ChCl/EG with 20 mM CuCl, (b) ChCl/EG with 20 mM CuCl₂, and (c) ChNO₃/EG with 20 mM Cu(NO₃)₂ at the given potentials in V_{Cu} . Insets: Plot of j against $t^{0.5}$ of the transients at $-0.3 V_{Cu}$ to determine diffusion coefficients for each electrolyte.

First, diffusion coefficients are determined by the Cottrell equation [Equation (2)] for the current transients at $-0.3 V_{Cu}$. D corresponds to the diffusion coefficient, c is the initial concentration of the analyte, and t is the time. The plots of current density vs. $t^{0.5}$ are shown together with a linear fit in the insets of Figures 7a–c. For ChCl/EG + CuCl, a diffusion coefficient of $2.6 \cdot 10^{-7} \text{ cm}^2 \text{ s}^{-1}$ is determined. This matches very well with values for Cu⁺ in chloride-containing DESs, which are in the range of $2.6\text{--}2.8 \cdot 10^{-7} \text{ cm}^2 \text{ s}^{-1}$.^[14,22,26,46] With CuCl₂, the calculated diffusion coefficient for Cu²⁺ is $1.4 \cdot 10^{-7} \text{ cm}^2 \text{ s}^{-1}$, also a value similar to those previously reported ($1.3\text{--}1.6 \cdot 10^{-7} \text{ cm}^2 \text{ s}^{-1}$).^[14,22,26,46] For the nitrate-based DES, a diffusion coefficient of $1.6 \cdot 10^{-7} \text{ cm}^2 \text{ s}^{-1}$ is obtained for Cu²⁺. This is slightly higher than the one with CuCl₂, albeit the difference is very small.

$$j = \frac{zFc\sqrt{D}}{\sqrt{\pi t}} \quad (2)$$

The current transients for the CuCl electrolyte (Figure 7a) exhibit a steep drop in cathodic current denoting the end of double-layer charging, followed by a slight rise and an exponential decay, typical for a three-dimensional nucleation and growth mechanism.^[47] Nuclei start forming and grow until the diffusion zones of adjacent nuclei become overlapping so that finally, the diffusion limit is approached. Comparing the curves, the maximum cathodic current increases, while the time at which the maximum occurs is shorter with rising overpotential. Focusing on the first second (Figure S9), one observes an additional peak with $-50 \mu\text{C cm}^{-2}$ (at $-0.1 V_{Cu}$) corresponding to the second part of Cu UPD. However, already at $-0.15 V_{Cu}$ it is only observable as a shoulder, and analysis is performed after the minimum of each transient focusing on bulk deposition. After a few seconds, the current in all systems approaches the same course over time independent of the applied potential due to diffusion limitation. This is also the case with CuCl₂ and Cu(NO₃)₂ (Figures 7b,c, and S10 for 40 s).

With CuCl₂ (Figure 7b), no current maximum is observable since the reduction of Cu²⁺ to Cu⁺ is occurring simultaneously to deposition. This formation of Cu⁺ causes a non-linear decay in current according to the Cottrell equation that exhibits a time-dependence of $t^{-0.5}$, since it is a diffusion-controlled reaction. This masks the initial rise and maximum in cathodic current due to deposition. As the potential step is large, the rate of Cu⁺ formation hardly changes with overpotential resulting in identical transients if only this process occurs. This is shown for transients at $0.4 V_{Cu}$ and $-0.05 V_{Cu}$ for 40 s (Figure S10), and even the one at $-0.1 V_{Cu}$ is very similar to those for the first 5 s before OPD starts. That independence of the reaction rate should be equally valid for even larger steps. Therefore, the reaction to Cu⁺ can be separated from deposition by subtracting the transient at $-0.05 V_{Cu}$ from the other ones before analysis, as done previously.^[21] Yet, it might be that UPD influences the progression of the transients.

For the Cu(NO₃)₂ electrolyte, it is assumed that the absence of a maximum in the current transients (Figure 7c) has the same reason. Based on the EQCM results, it is known that if the deposition takes place in two steps via Cu⁺, the second directly follows the first. For that reason, these processes are not separated. Also, UPD is not observable as a separate process but if at all as a shoulder, approximately before 0.3 s.

For the initial stages of Cu deposition, the current transients in all electrolytes are analyzed according to the model of Scharifker and Mostany.^[48,49] Further details on the fitting procedure are given in the experimental section. The model describes the time evolution of the current density for three-dimensional nucleation with diffusion-limited growth [Equation (3)]. It is fitted directly to the transients in the case of CuCl and Cu(NO₃)₂ and is fitted to processed data, as described previously, for CuCl₂. N_0 is the number density of active nucleation sites, A is the nucleation rate constant, and k can be

calculated with Equation (4), with M being the molar mass and ρ the density of the deposit.

$$j = \frac{zFc\sqrt{D}}{\sqrt{\pi t}} \left[1 - \exp \left\{ -N_0\pi kD \left(t - \frac{1 - \exp(-At)}{A} \right) \right\} \right] \quad (3)$$

$$k = \frac{4}{3} \sqrt{\frac{8\pi cM}{\rho}} \quad (4)$$

So far, this model has been used to analyze Cu deposition from various aqueous systems^[27,50–52] as well as from non-aqueous electrolytes, e.g. for Ni deposition.^[53] Electrodeposition kinetics for DES baths has so far been analyzed by the Scharifker-Hills model.^[14,18,19] Compared to this model,^[54,55] Equation (3) is a more general approach and instantaneous and progressive nucleation can be considered as limiting cases.^[48,56] If A is very large ($A \rightarrow \infty$), nucleation is instantaneous since all nuclei are formed at the same time. Subsequently, the parameter α [Equation (5)] approaches zero ($\alpha \rightarrow 0$), and Equation (3) simplifies to Equation (6).^[47,48,53] By contrast, nucleation is progressive if α is very large ($\alpha \rightarrow \infty$). Another characteristic value is the saturation number density N_s [Equation (7)].

$$\alpha = \frac{N_0\pi kD}{A} \quad (5)$$

$$j = \frac{zFc\sqrt{D}}{\sqrt{\pi t}} [1 - \exp(-N_0\pi kDt)] \quad (6)$$

$$N_s = \sqrt{\frac{AN_0}{2kD}} \quad (7)$$

For the CuCl-containing electrolyte, the transients are fitted to Equation (3) resulting in values for A between 3.8 and 304 s⁻¹, increasing for more negative overpotentials. Thus, the deposition approaches the instantaneous nucleation and growth mechanism, which is expected for large overpotentials.^[27] However, as α is close to zero (0.02–0.1), nucleation is rather instantaneous in all cases. A and N_s increase exponentially with overpotential (Figure S11), complying with the theory of three-dimensional diffusion-controlled nucleation and growth.^[27,48] The value at $-0.125 V_{Cu}$ does not fit into the series but the curve of $\ln(A)$ vs. $-E$ (Figure S11a) may exhibit a larger slope for lower overpotentials. As the slope depends on the size of a critical copper nucleus,^[50] it could be that for increasing overpotential, fewer atoms are needed to form a critical cluster, which serves as a stable nucleus for further spontaneous growth. This dependence has been observed in different systems.^[57,58] The density of active sites increases with overpotential (Table 1), as expected. Deposition in the CuCl₂- and Cu(NO₃)₂-containing DESs follows instantaneous nucleation in all cases, as A is extremely high and α close to zero, so Equation (6) is fitted to the transients. The resulting values for N_0 are given in Table 1. In a similar DES consisting of ChCl/EG + 20 mM CuCl₂·2H₂O on a Pt electrode, progressive nucleation was found but for a lower overpotential.^[14] A change in mechanism from progressive to instantaneous with increasing

Table 1. Number density of active nucleation sites N_0 given in 10⁶ cm⁻² for various potentials during Cu deposition on Au(111).

E [V _{Cu}]	ChCl/EG + CuCl	ChCl/EG + CuCl ₂	ChNO ₃ /EG + Cu(NO ₃) ₂
-0.125	1		8
-0.15	10	15	15
-0.175	19		22
-0.2	33	49	33
-0.225	50		39
-0.25	72	79	46
-0.275	89		52
-0.3	88	107	58
-0.35	145		75
-0.4	186	178	68

overpotential during copper deposition was found in a ChCl/urea DES with 50 mM CuCl₂^[18] and in a ChCl/EG DES with 10 mM CuCl₂.^[21]

The number density of active nucleation sites N_0 (Table 1) is similar for both chloride-containing DESs and the Cu(NO₃)₂ electrolyte at potentials above $-0.225 V_{Cu}$, further indicating that deposition proceeds similarly. The fact that with CuCl₂ and Cu(NO₃)₂ the nucleation seems to be instantaneous also for lower overpotentials might be explained by imperfect fitting at the very beginning of deposition due to UPD or Cu⁺ formation. That N_0 is smaller at larger overpotential in the Cu(NO₃)₂ than in the chloride-containing DESs could be attributed to a side reaction blocking nucleation sites. The existence of this irreversible process is suspected from the cyclic voltammogram (Figure 3b). Nevertheless, N_0 increases with the increase of the applied overpotential in all cases, as expected and observed in other systems.^[27,50–52] The obtained values for N_0 themselves are of the same orders of magnitude compared to those for copper deposition in aqueous electrolytes.^[27,50–52]

Conclusion

In this study, copper deposition onto Au(111) was investigated from DESs type III, namely mixtures of choline chloride or choline nitrate with ethylene glycol. The aim was to elaborate on the differences in deposition with salts consisting of Cu²⁺ or Cu⁺ cations in combination with chloride or nitrate anions. Cu bulk deposition is preceded by Cu UPD occurring in the chloride-based electrolytes in two steps approximately 600 mV apart from each other. This behavior is comparable to that of chloride-containing aqueous and other non-aqueous electrolytes and is probably influenced by chloride adsorption. UPD also occurs in the nitrate-based DES, in contrast to aqueous media.

Employing cyclic voltammetry and EQCM, it was shown for the chloride-based DESs, both with CuCl and CuCl₂, that Cu is selectively deposited from Cu⁺ and dissolved to Cu⁺. At more positive potentials, the Cu⁺/Cu²⁺ redox wave is detected, followed by chloride-induced Au dissolution. Therefore, with CuCl₂, Cu⁺ formation starts roughly 800 mV positive of the Cu⁺/Cu⁰ redox potential and is steadily generated at lower potentials. The large separation between the formation and

deposition of Cu^+ is due to the strong stabilization of Cu^+ species by chloride anions, which is also the reason for the comproportionation. Despite the similarities for Cu deposition with water and EG as solvents, it might be influenced by the presence of EG acting as an inhibitor, similar to PEG. With choline nitrate in exchange for chloride, the $\text{Cu}^+/\text{Cu}^{2+}$ redox process is directly followed by bulk deposition. The deposition involves two electrons in total and consists of two single electron transfer reactions with Cu^+ as intermediate. The reverse is also true for dissolution. In addition, dissolution occurs via comproportionation to Cu^+ , implying that Cu^+ is stabilized by nitrate anions in the DES. However, deposition and dissolution in this electrolyte occur several hundred mV more positively than in the chloride-based DESs, as seen with an Ag/AgCl reference electrode. The stabilizing effect of Cu^+ in the DES is much more pronounced with chloride than with nitrate anions. Thus, the high stability of Cu^+ in the presence of chloride compared to nitrate in a choline-based DES with ethylene glycol is evident.

The nucleation and growth mechanism of the DESs was investigated by chronoamperometric measurements and analyzed by the model of Scharifker and Mostany. This versatile approach was applied for the first time to study the electro-deposition of copper from DESs. A diffusion-controlled, three-dimensional nucleation and growth mechanism is demonstrated for all DESs, and nucleation is virtually instantaneous for all overpotentials studied. Consequently, there is no significant difference between chloride and nitrate anions in affecting the nucleation and growth mechanism of Cu onto Au(111).

Experimental Section

The DESs were prepared by mixing a choline salt with an HBD and if required, with a copper salt under N_2 atmosphere ($\text{H}_2\text{O} < 0.5$ ppm, $\text{O}_2 < 0.5$ ppm) in a glovebox (M. Braun, Garching, Germany). After stirring at 80°C until a homogeneous liquid was obtained, the DESs were dried at 10^{-1} to 10^{-3} mbar. The composition of the DESs is ChCl/EG 1:2 ($x_{\text{ChCl}} = 0.33$) and ChNO_3/EG 1:2 ($x_{\text{ChNO}_3} = 0.33$). Choline chloride (Alfa Aesar, 98 + %) was recrystallized twice from absolute ethanol (Merck, 99.9%). Choline nitrate was prepared from choline hydroxide solution (Sigma Aldrich, 46 wt.% in H_2O) by adding HNO_3 (Merck, 65%).^[59] Subsequently, it was dried under vacuum and recrystallized from absolute ethanol. Ethylene glycol (Sigma Aldrich, 99.8%) was used as received. Copper(II) chloride dihydrate (Merck, 99 + %) was dehydrated under vacuum before usage, whereas copper(I) chloride (Sigma Aldrich, 99.995 + %) and copper(II) nitrate trihydrate (Merck, 99,5 + %) were used as received.

The cyclic voltammetry and chronoamperometry measurements were carried out in the above-mentioned glovebox at room temperature using a cell with a volume of 0.25 cm^3 made of Kel-FTM. An IM6 (Zahner-Elektrik, Kronach, Germany) and Interface 1010B (Gamry Instruments, Warminster, United States) were used as potentiostats for cyclic voltammetry and chronoamperometry, respectively. As a working electrode, an Au(111) single crystal of 12 mm diameter (MaTeCK, Jülich, Germany) and as counter and reference electrodes, a Pt and a Cu wire (MaTeCK) were used, respectively. With the Cu wire in the Cu salt solution as a reference electrode, UPD can be easily distinguished from OPD. However, since the reference potential is set by Cu deposition/dissolution, whose potential depends on the anions, one cannot compare the

absolute peak positions in different DESs. In a typical cyclic voltammetry experiment, less than 1% of copper ions in the solution were consumed during the deposition. This results in a shift of the equilibrium potential for Cu deposition of less than 1 mV. For example, during the deposition from the $\text{ChCl}/\text{EG} + 20\text{ mM CuCl}$ DES (red curve in Figure 3a) -5.6 mCcm^{-2} , which corresponds to 0.9% of copper ions present, are consumed. Thus, the potential shift equals 0.3 mV according to the Nernst equation. Therefore, the Cu wire can be considered a stable Cu reference electrode for the systems under investigation.

EQCM measurements were performed in the glovebox on an Au-coated 5 MHz quartz crystal in a temperature-controlled cell at 40°C to compensate for the high viscosity of the DESs. For this purpose, a QCM-D (MicroVacuum, Budapest, Hungary) in combination with an Interface 1010E potentiostat (Gamry Instruments) was used. For the cyclic voltammetry coupled with EQCM, a leak-free Ag/AgCl reference electrode (MicroVacuum) and a Cu wire as counter electrode were used. For the chronopotentiometric EQCM measurements, Cu wires were used as reference and counter electrodes. The AT-cut quartz crystal (MicroVacuum) was coated with gold in a Q150 GB sputter coater (Quorum Technologies, Laughton, United Kingdom). The area in contact with the electrolyte was 0.324 cm^2 .

For the analysis of the chronoamperometry measurements, the current transients are fitted to the model of Scharifker and Mostany. For the $\text{ChCl}/\text{EG} + \text{CuCl}$ electrolyte, the fit is performed without further processing of the data after the minimum of each transient focusing on bulk deposition. With $\text{ChCl}/\text{EG} + \text{CuCl}_2$, a current transient at $-0.05\text{ V}_{\text{Cu}}$ is subtracted from each transient in the OPD region, as explained previously. This results in a maximum in current density, like in the CuCl electrolyte, occurring at shorter times with increasing overpotential. The fit is performed starting at 0.3 s for the transient at $-0.15\text{ V}_{\text{Cu}}$, down to 0.06 s for the transient at $-0.4\text{ V}_{\text{Cu}}$, which is in all cases approximately the time at which the maximum occurs. With $\text{ChNO}_3/\text{EG} + \text{Cu}(\text{NO}_3)_2$, also no current maximum is observable but the $\text{Cu}^{2+}/\text{Cu}^+$ reaction cannot be nicely separated from OPD. Therefore, the raw data is fitted from a time at which the maximum must already have occurred, according to comparison with the other electrolytes. This is 3 s for the transient at $-0.125\text{ V}_{\text{Cu}}$, 2 s for $-0.15\text{ V}_{\text{Cu}}$, 1.5 s for $-0.175\text{ V}_{\text{Cu}}$, and 1 s for the other transients. All curves in all electrolytes are fitted until $t = 5\text{ s}$. For CuCl, the curves are fitted with a coefficient of correlation $R^2 > 99.5\%$, and for CuCl_2 as well as $\text{Cu}(\text{NO}_3)_2$ with $R^2 > 97\%$. A comparison of the current transients in the case of CuCl and $\text{Cu}(\text{NO}_3)_2$ and of the processed data for CuCl_2 with the fitted curves is provided in Figure S12 for all analysed overpotentials.

Acknowledgements

This research was conducted as part of the German Research Foundation (DFG) under Project ID 390874152 (POLiS Cluster of Excellence) as well as the Schwerpunktprogramm (priority program) SPP-2248 "Polymer-based Batteries" under Project ID 441209207. Further, support by the BMBF through the InnoSüd-project (Grant Agreement: 03IH5024D) is gratefully acknowledged. Open Access funding enabled and organized by Projekt DEAL.

Conflict of Interest

The authors declare no conflict of interest.

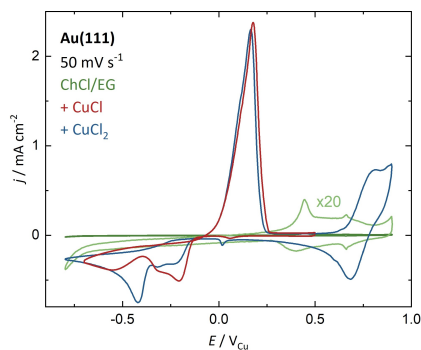
Keywords: Au single crystal · Cu deposition · deep eutectic solvent · EQCM · non-aqueous electrolyte

- [1] S. Miura, H. Honma, *Surf. Coat. Technol.* **2003**, 169–170, 91–95.
- [2] T. Kobayashi, J. Kawasaki, K. Mihara, H. Honma, *Electrochim. Acta* **2001**, 47, 85–89.
- [3] W.-P. Dow, M.-Y. Yen, S.-Z. Liao, Y.-D. Chiu, H.-C. Huang, *Electrochim. Acta* **2008**, 53, 8228–8237.
- [4] K. Kondo, R. N. Akolkar, D. P. Barkey, M. Yokoi, *Copper Electrodeposition for Nanofabrication of Electronics Devices*, Springer, New York, **2014**, Vol. 171.
- [5] R. Bernasconi, M. Zabarjadi, L. Magagnin, *J. Electroanal. Chem.* **2015**, 758, 163–169.
- [6] J. R. Bezerra-Neto, N. G. Sousa, L. P. M. Dos Santos, A. N. Correia, P. de Lima-Neto, *Phys. Chem. Chem. Phys.* **2018**, 20, 9321–9327.
- [7] A.-M. J. Popescu, V. Constantin, A. Cojocaru, M. Olteanu, *Rev. Chim.* **2011**, 62, 206–211.
- [8] N. Batina, T. Will, D. Kolb, *Faraday Discuss.* **1992**, 94, 93–106.
- [9] H. Matsumoto, I. Oda, J. Inukai, M. Ito, *J. Electroanal. Chem.* **1993**, 356, 275–280.
- [10] F. Endres, A. Schweizer, *Phys. Chem. Chem. Phys.* **2000**, 2, 5455–5462.
- [11] E. L. Smith, A. P. Abbott, K. S. Ryder, *Chem. Rev.* **2014**, 114, 11060–11082.
- [12] A. P. Abbott, G. Capper, D. L. Davies, H. L. Munro, R. K. Rasheed, V. Tambyrajah, *Chem. Commun.* **2001**, 19, 2010–2011.
- [13] A. P. Abbott, G. Capper, D. L. Davies, R. K. Rasheed, V. Tambyrajah, *Chem. Commun.* **2003**, 1, 70–71.
- [14] A. P. Abbott, K. El Ttaib, G. Frisch, K. J. McKenzie, K. S. Ryder, *Phys. Chem. Chem. Phys.* **2009**, 11, 4269–4277.
- [15] M. U. Cebelin, S. Zeller, B. Schick, L. A. Kibler, T. Jacob, *ChemElectroChem* **2019**, 6, 141–146.
- [16] P. Sebastián, E. Vallés, E. Gómez, *Electrochim. Acta* **2013**, 112, 149–158.
- [17] Y. Su, J. Liu, R. Wang, S. Aisa, X. Cao, S. Li, B. Wang, Q. Zhou, *J. Electrochem. Soc.* **2018**, 165, H78–H83.
- [18] P. Sebastián, E. Vallés, E. Gómez, *Electrochim. Acta* **2014**, 123, 285–295.
- [19] P. Sebastián, E. Torralba, E. Vallés, A. Molina, E. Gómez, *Electrochim. Acta* **2015**, 164, 187–195.
- [20] P. Sebastián, E. Gómez, V. Climent, J. M. Feliu, *Electrochem. Commun.* **2017**, 78, 51–55.
- [21] Z. Tan, S. Liu, J. Wu, Z. Nan, F. Yang, D. Zhan, J. Yan, B. Mao, *ChemElectroChem* **2022**, 9, e202101412.
- [22] T. Geng, S. J. Zeller, L. A. Kibler, M. U. Cebelin, T. Jacob, *ChemElectroChem* **2022**, 9, e202101283.
- [23] E. Herrero, L. J. Buller, H. D. Abruña, *Chem. Rev.* **2001**, 101, 1897–1930.
- [24] Z. Shi, S. Wu, J. Lipkowski, *Electrochim. Acta* **1995**, 40, 9–15.
- [25] Z. Shi, S. Wu, J. Lipkowski, *J. Electroanal. Chem.* **1995**, 384, 171–177.
- [26] D. Lloyd, T. Vainikka, L. Murtomäki, K. Kontturi, E. Ahlberg, *Electrochim. Acta* **2011**, 56, 4942–4948.
- [27] A. Ramos, M. Miranda-Hernández, I. González, *J. Electrochem. Soc.* **2001**, 148, C315.
- [28] C. T. J. Low, C. Ponce de Leon, F. C. Walsh, *Trans. IMF* **2015**, 93, 74–81.
- [29] W. Shao, G. Pattanaik, G. Zangari, *J. Electrochem. Soc.* **2007**, 154, D201–D207.
- [30] H. F. Alesary, H. K. Ismail, A. H. Odda, M. J. Watkins, A. A. Majhool, A. D. Ballantyne, K. S. Ryder, *J. Electroanal. Chem.* **2021**, 897, 115581.
- [31] M. Y. Gao, C. Yang, Q. B. Zhang, Y. W. Yu, Y. X. Hua, Y. Li, P. Dong, *Electrochim. Acta* **2016**, 215, 609–616.
- [32] S. Ghosh, S. Roy, *Surf. Coat. Technol.* **2014**, 238, 165–173.
- [33] S. Ghosh, K. Ryder, S. Roy, *Trans. IMF* **2014**, 92, 41–46.
- [34] A. Y. M. Al-Murshedi, J. M. Hartley, A. P. Abbott, K. S. Ryder, *Trans. Inst. Met. Finish.* **2019**, 97, 321–329.
- [35] P. E. Valverde, T. A. Green, S. Roy, *J. Appl. Electrochem.* **2020**, 50, 699–712.
- [36] T. A. Green, P. Valverde, S. Roy, *J. Electrochem. Soc.* **2018**, 165, D313–D320.
- [37] C. Köntje, L. A. Kibler, D. M. Kolb, *Electrochim. Acta* **2009**, 54, 3830–3834.
- [38] W. O. Karim, S. B. Aziz, M. A. Brza, R. M. Abdullah, M. F. Z. Kadir, *Appl. Sci.* **2019**, 9, 4401.
- [39] M. B. Vukmirovic, R. R. Adzic, R. Akolkar, *J. Phys. Chem. B* **2020**, 124, 5465–5475.
- [40] M. Lundström, J. Aromaa, O. Forsén, *Hydrometallurgy* **2009**, 95, 285–289.
- [41] H. Zhao, J. Chang, A. Boika, A. J. Bard, *Anal. Chem.* **2013**, 85, 7696–7703.
- [42] Z. V. Feng, X. Li, A. A. Gewirth, *J. Phys. Chem. B* **2003**, 107, 9415–9423.
- [43] G. Sauerbrey, *Z. Phys.* **1959**, 155, 206–222.
- [44] D. Aurbach, M. Moshkovich, *J. Electrochem. Soc.* **1998**, 145, 2629–2639.
- [45] M. Peykova, E. Michailova, D. Stoychev, A. Milchev, *Electrochim. Acta* **1995**, 40, 2595–2601.
- [46] D. Shen, K. Steinberg, R. Akolkar, *J. Electrochem. Soc.* **2018**, 165, E808–E815.
- [47] D. Pletcher, R. Greff, R. Peat, L. M. Peter, J. Robinson, *Instrumental Methods in Electrochemistry*, Woodhead Publishing, Cambridge, **2011**.
- [48] B. R. Scharifker, J. Mostany, *J. Electroanal. Chem.* **1984**, 177, 13–23.
- [49] B. R. Scharifker, J. Mostany, M. Palomar-Pardavé, I. González, *J. Electrochem. Soc.* **1999**, 146, 1005–1012.
- [50] M. Palomar-Pardavé, I. González, N. Batina, *J. Phys. Chem. B* **2000**, 104, 3545–3555.
- [51] D. Grujicic, B. Pesic, *Electrochim. Acta* **2005**, 50, 4426–4443.
- [52] O. Ghodbane, L. Roué, D. Bélanger, *Electrochim. Acta* **2007**, 52, 5843–5855.
- [53] O. Mann, W. Freyland, *J. Phys. Chem. C* **2007**, 111, 9832–9838.
- [54] G. Gunawardena, G. Hills, I. Montenegro, B. R. Scharifker, *J. Electroanal. Chem.* **1982**, 138, 225–239.
- [55] B. R. Scharifker, G. Hills, *Electrochim. Acta* **1983**, 7, 879–889.
- [56] M. Y. Abyaneh, M. Fleischmann, *Electrochim. Acta* **1982**, 27, 1513–1518.
- [57] J.-J. Lee, B. Miller, X. Shi, R. Kalish, K. A. Wheeler, *J. Electrochem. Soc.* **2001**, 3, C183–C190.
- [58] T. Jiang, M. J. Chollier Brym, G. Dubé, A. Lasia, G. M. Brisard, *Surf. Coat. Technol.* **2006**, 201, 10–18.
- [59] E. G. Blackett, A. J. Soliday, *United States Patent Office, US2774759* **1956**.

Manuscript received: September 19, 2021
Revised manuscript received: June 24, 2022
Accepted manuscript online: June 29, 2022

RESEARCH ARTICLE

Cu electrodeposition onto Au(111) is studied in deep eutectic solvents (DESs) type III with choline chloride or nitrate and ethylene glycol. Underpotential deposition is observable in all DESs. Cu^+ is stabilized more by Cl^- than by NO_3^- and with Cl^- being present, the deposition involves one electron, whereas it proceeds in two consecutive steps with NO_3^- . A diffusion-controlled, three-dimensional nucleation and growth mechanism is found.



*T. Geng, B. W. Schick, M. Uhl,
Prof. Dr. A. J. C. Kuehne, Dr. L. A. Kibler,
Dr. M. U. Cebelin*, Prof. Dr. T. Jacob**

1 – 12

**Influence of Chloride and Nitrate
Anions on Copper Electrodeposition
onto Au(111) from Deep Eutectic
Solvents**

